

# Fast-Ion-Driven MHD Instabilities and Consequent Fast Ion Losses in the Compact Helical System

M. Isobe 1), K. Toi 1), K. Nagaoka 1), C. Suzuki 1), K. Goto 2), T. Akiyama 1),  
T. Minami 1), S. Murakami 3), N. Nakajima 1), S. Nishimura 1), M. Nishiura 1),  
A. Shimizu 1), S. Yamamoto 4), Y. Yoshimura 1), M. Sasao 5), K. Matsuoka 1),  
S. Okamura 1), D.A. Spong 6)

1) National Institute for Fusion Science, Toki 509-5292 Japan

2) Nagoya University, Nagoya 464-8603 Japan

3) Kyoto University, Kyoto 606-8501 Japan

4) Osaka University, Suita 565-0871 Japan

5) Tohoku University, Sendai 980-8579 Japan

6) Oak Ridge National Laboratory, Oak Ridge TN 27830-6169 USA

e-mail contact of main authors : isobe.mitsutaka@LHD.nifs.ac.jp

**Abstract.** Impacts of fast-ion-driven MHD modes on fast ion transport have been investigated in a medium size helical device CHS having negative magnetic shear over an entire region of plasma. Recently, it was observed that bursting toroidicity-induced Alfvén eigenmodes (TAEs) excited by co-circulating beam ions enhance beam ion loss at low magnetic field strength of 0.9 T. Flux of escaping beam ions steeply increases as the magnetic fluctuation level increases. Excitation of energetic particle modes (EPMs) due to co-circulating beam ions has been also observed in CHS, of which frequency range is located appreciably below the TAE gap frequency. Bursts of EPMs and TAEs recur periodically accompanied with periodically increased beam ion loss. Fast particle diagnostics indicate that beam ions transported by these modes are promptly lost to the large major radius side of CHS plasma in the horizontally elongated section. Particle simulation suggests that a perturbed magnetic field whose amplitude is consistent with the CHS experiment can rapidly increase the fast ion loss.

## 1. Introduction

Interaction between energetic ions and kinetically driven magnetohydrodynamics (MHD) modes is one of the key physics issues in current fusion experiments. In particular, the energetic particle modes (EPMs) [1] and Alfvén eigenmodes (AEs) [2] may lead to redistribution and/or anomalous loss of energetic alpha particles produced by the deuterium-tritium (d-t) reaction in a future burning plasma [3]. Anomalous loss of alpha particles should

be avoided because it results in losing a self-ignition condition. In addition, localized heat load on the first wall due to impact of escaping alpha particles may give serious damage to the device. Therefore, excitation of the modes sensitively dependent on fast ion distribution in real and velocity spaces and rotational transform profile  $1/q$ , and effects of the modes on fast ion confinement have been intensively studied in many tokamaks such as JET, TFTR and JT-60U [4-8]. The MHD instabilities mentioned above have been also observed in helical/stellarator devices, e.g. CHS, LHD and W7-AS, which offer an alternative concept for a magnetic confinement fusion reactor [9-12]. In this paper, we report recent results on fast-ion-driven MHD instabilities and their influences on fast ion transport in the Compact Helical System (CHS) using several fast ion diagnostics with improved performance. The magnetic configuration of CHS has negative magnetic shear over an entire region of plasma, introducing shear Alfvén continua different from tokamaks. In our experiment, fast ions who play a key role in driving MHD instabilities are generated in a plasma by injecting fast-neutral beams (NBs) as a substitute for alpha particles. We describe the experimental setup for this work in Section 2. In Section 3, experimental results on fast-ion-driven MHD instabilities and their effects on fast ion transport are presented. Results from particle simulation taking a perturbed magnetic field into account are presented in Section 4. Finally, the summary is briefly given in Section 5.

## 2. CHS experimental setup

The CHS is a medium-sized helical device having device major radius of 1 m and averaged plasma minor radius of  $\sim 0.2$  m and is featured by its low aspect ratio of 5. Because of the low aspect ratio and non-axisymmetric magnetic field, an issue on fast ion orbit is one of key physics subjects. The arrangement of NB injectors and fast particle diagnostics important for this work are shown in Figure 1. The CHS is equipped with two NB injectors (NB#1 of 40 kV/0.8 MW, NB#2 of 32 kV/0.8 MW). Hydrogen NBs are tangentially co-injected into hydrogen plasmas in our case. The fast ion experiment in CHS is characterized by the combination of a variety of fast particle diagnostics, i.e. scintillator-based lost fast ion probes (SLIP) [13], Faraday film-based lost fast ion probe (FLIP) [14], a directional

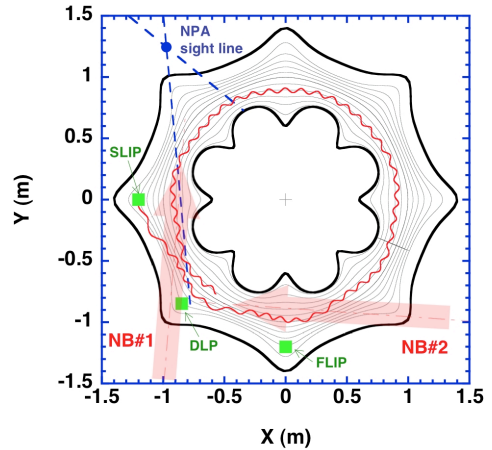


FIG. 1. Arrangement of neutral beam injectors and fast particle diagnostics on CHS. The red solid line shows an example of orbit of fast ion (38 keV) reaching the SLIP in  $B_t/R_{ax}$  of 0.9 T/0.974 m.

Langmuir probe [15] and a charge exchange (CX) neutral particle analyzer (NPA) whose viewing angle is horizontally variable [16]. The SLIP and FLIP are capable of measuring energy and pitch-angle of escaping fast ions simultaneously. Array of detectors measuring H $\alpha$  light emission is also used to obtain valuable information on energetic ion behavior. In regard to the magnetic fluctuation measurement, toroidal and poloidal sets of the Mirnov coil arrays placed outside of plasma are employed in this study. Fast ion experiments in CHS were performed using hydrogen plasmas with the following parameters : the toroidal magnetic field strength  $B_t = 0.9\sim 1.4$  T, electron density  $n_e = (0.5\sim 2)\times 10^{19}$  m $^{-3}$ , injection energy of H $^0$  beam  $E_b = 30\sim 39$  keV and  $v_{b//}/v_A = 0.35\sim 0.48$ , which is the ratio of the beam ions' velocity parallel to the Alfvén velocity.

### 3. Experimental results

#### 3.1 EPMs and Alfvén eigenmodes observed in CHS

Figure 2 shows typical time traces of the discharge where fast-ion-driven modes are destabilized in  $B_t/R_{ax}$  of 0.91 T/0.962 m, (a) co-flowing net plasma current dominated by Ohkawa current, (b)  $dB_\theta/dt$ , (c) magnetic spectrogram, (d) line-averaged  $n_e$  and (e)  $v_{b//}/v_A$  when two NBs with total port-through NB power  $P_{nb}$  of 1.6 MW are tangentially co-injected. In the former half of discharge ( $t < 105$  ms), repetitive bursting magnetic fluctuations are seen. This mode is revealed to be  $n=2/m=3$ , where  $n$  and  $m$  stand for the toroidal and poloidal mode numbers, rotating in the ion-diamagnetic direction. It shows rapid frequency downshift from  $\sim 100$  kHz to  $\sim 40$  kHz with a time scale of  $\sim 1$  ms. This

instability is not seen in high  $n_e$  regime, i.e., low beam  $\beta$  regime. As  $n_e$ , in other words,  $v_{b//}/v_A$  increases, the bursting modes having  $f < 100$  kHz disappear and weaker fluctuations having higher frequency ( $f > 100$  kHz) become intense in turn. The higher frequency modes are strongly destabilized when the condition of  $v_{b//}/v_A > 1/3$  is fulfilled. Here  $v_A$  is evaluated from line-averaged  $n_e$  and effective ion charge is assumed to be  $Z_{eff}$ . The mode numbers are

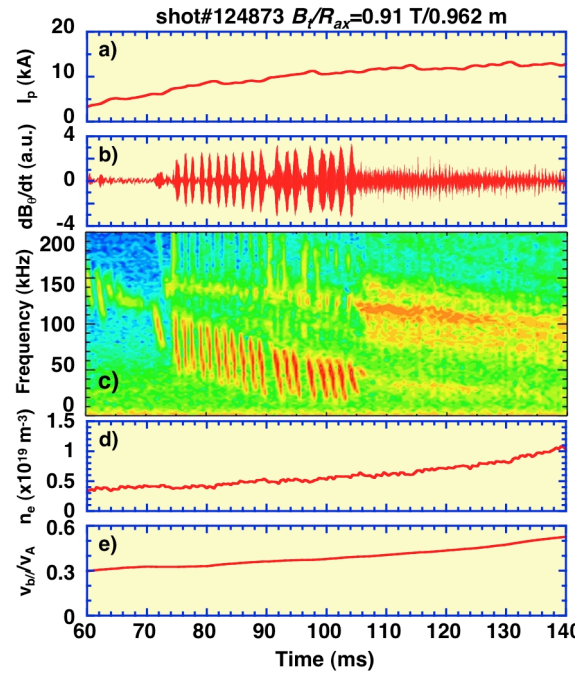


FIG. 2. Fast-ion-driven MHD instabilities observed in outward shifted configuration ( $R_{ax}=0.962$  m) of CHS at low  $B_t$  (0.91 T). (a) net plasma current, (b)  $dB_\theta/dt$ , (c) magnetic spectrogram, (d) line-averaged  $n_e$  and (e)  $v_{b//}/v_A$ .

measured to be  $n=1/m\sim 2$ . This mode also propagates in the ion-diamagnetic direction. As for this discharge, the rotational transform and shear Alfvén continua for the  $n=1$  and  $n=2$  modes are shown in Figure 3. The frequency of repetitive bursting modes accompanied with the

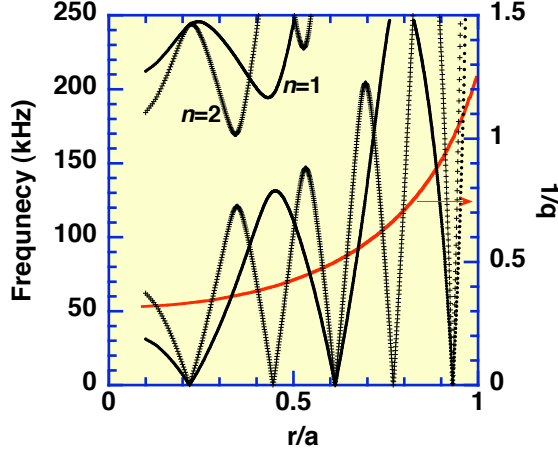


FIG. 3. Shear Alfvén continua (2D) for  $n=1$  and 2 modes and rotational transform ( $1/q$ ) where  $q$  is the safety factor for  $R_{ax} = 0.962$  m. Only poloidal mode coupling is taken into account and  $n_e(0)$  is  $1.0 \times 10^{19} \text{ m}^{-3}$  in this calculation.  $Z_{eff}$  is assumed to be 3.

experimental parameter range suggests that the observed mode with  $f > 100$  kHz is  $n=1$  TAE. Also, the condition of the sideband excitation, i.e.  $v_{b//}/v_A > 1/3$  is satisfied in this case. In the CHS configuration, the rotational transform increases towards the plasma edge. Because of this, the TAE gap does not expand to the edge region, suggesting that the mode would be core-localized in CHS.

### 3.2 TAE-induced fast ion transport

Impact of TAE instabilities on fast ion transport is of great concern. In the previous experiment with a single NB heating, significant transport and/or loss of fast ions by TAEs were not observed. This is probably due to the low amplitude of excited fluctuation ( $\delta B_\theta < 10^{-5}$  T at the Mirnov coil position) [10]. The recent experiments reveal that repetitive anomalous losses of fast ions are significantly induced due to  $n=1$  TAEs; the gap for these modes is formed by a coupling of  $m=2$  and 3 poloidal modes and results in  $\delta B_\theta$  over  $10^{-5}$  T when two NBs are tangentially co-injected. Figure 4 shows enlarged waveforms of the TAE shot shown in Figure 2, together with the poloidal cross section of CHS where measurements are carried out. Correlated with the TAE bursts of  $\delta B_\theta \sim 2 \times 10^{-5}$  T at the Mirnov coil position, lost fast ion probes placed at the large major radius side of horizontally elongated cross section show periodic increase of flux of lost fast ion of which energy is close to beam

rapid frequency downshift in the time range of  $t < 105$  ms is located at the inside of Alfvén continua, where the strong damping effect is expected. In addition, the  $m$  number is specifically identified without mixing for this instability. Therefore, we may reasonably conclude that observed bursting modes are the so-called EPMs. In regard to MHD instabilities having higher frequency ( $f > 100$  kHz) appeared in  $t > 105$  ms, it is thought to be core-localized TAEs [11] for the following reasons. The shear Alfvén spectrum calculated with the

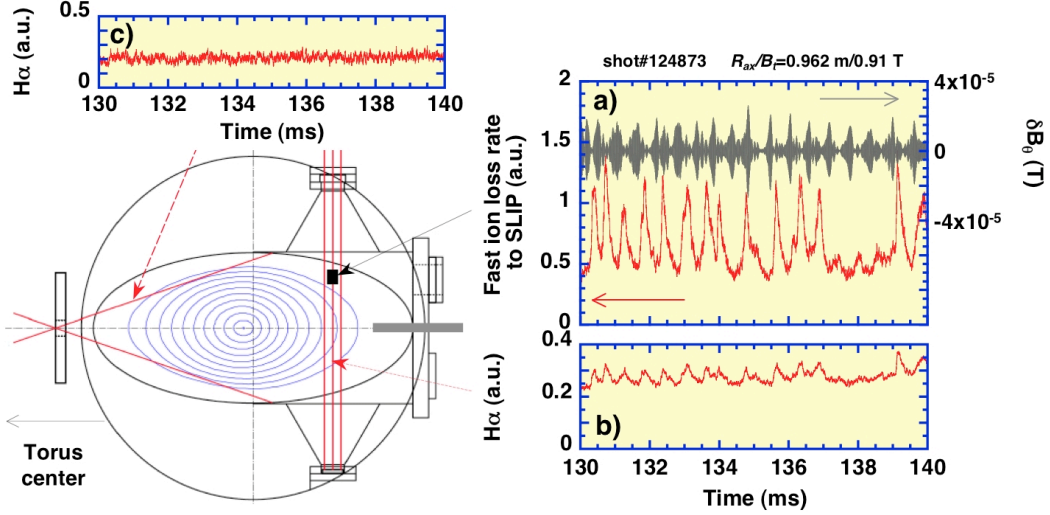


FIG. 4. Waveforms of TAE shot in  $R_{ax}/B_t$  of 0.962 m/0.91 T, which is the same as that shown in Figure 2. (a) amplitude of magnetic fluctuation in Tesla measured with the Mirnov coil placed outside the plasma. The signal is filtered in the range from 95 kHz to 120 kHz. (b)  $H\alpha$  light emissivity in  $r/a > 0.9$  at the outboard side. (c)  $H\alpha$  light emissivity in  $r/a > 0.9$  at the inboard side.

injection energy  $E_b$ , indicating that the beam ions are expelled due to the TAE bursts. From the pitch-angle of lost fast ions measured with the SLIP and the following orbit calculation, we identify that lost fast ions have co-going transit orbit which deviates substantially from magnetic flux surfaces to the outboard side. The time trace of  $H\alpha$  light emissivity at the same diagnostic port but different toroidal angle behaves like fast ion probes' signal. The periodic increases of  $H\alpha$  light emissivity at the outboard side (Fig. 4b) are thought to be due to the

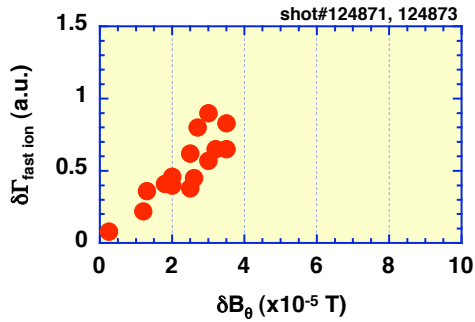


FIG. 5. Fast ion loss flux ( $\delta \Gamma_{\text{fast ion}}$ ) evaluated from the SLIP as a function of amplitude of  $\delta B_\theta$  measured with the magnetic probe placed outside the plasma for the TAE shots.

impact of fast ions transported to the peripheral domain onto the neutral hydrogen gas existing densely at the periphery. Meanwhile, no remarkable change in  $H\alpha$  emissivity at the edge region of the inboard side is seen (Fig. 4c). These observations tell us that co-going transit beam ions are transported to the outboard side resulting from the TAE bursts and are lost. CX fast neutrals have been also measured with the NPA in this experiment. However, because of the poor time resolution (0.2 ms) of the system, periodic

changes of fast neutral flux associated with the above-shown TAE bursts having shorter time interval than the time resolution were not clearly followed. Fluxes of lost fast ions when the TAE activities are destabilized are dependent on  $\delta B_\theta$ . Figure 5 shows fast ion loss rate to the probe as a function of  $\delta B_\theta$ . It is seen that fast ion loss flux increases as  $\delta B_\theta$  increases.

### 3.3. Impact of EPM on fast ion transport

Figure 6 shows the time traces of (a)  $dB_\theta/dt$ , (b) fluxes of CX fast neutral particles having the energy of 39.1 keV, (c) SLIP signal originating from lost fast ions having energy close to  $E_b$ , and (d)  $H\alpha$  light emissivity while EPM bursts with the mode number of  $n=2/m=3$  are excited

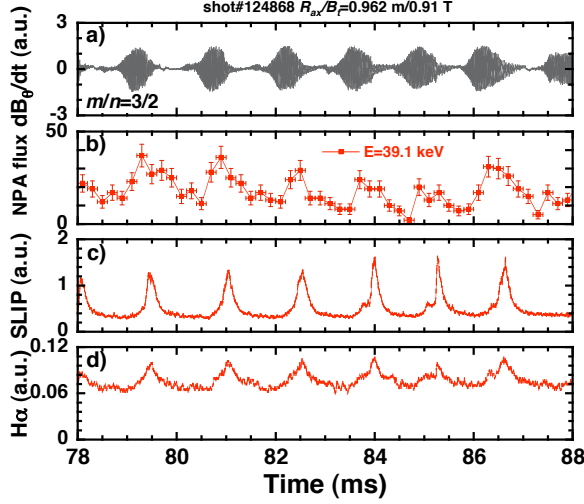


FIG. 6. Time evolution of (a)  $dB_\theta/dt$ , (b) fast neutral flux measured with NPA set to be tangential, (c) lost fast ion flux measured with the SLIP and (d)  $H\alpha$  light emissivity measured at the outboard side of the torus.

by co-circulating beam ions in a low density plasma ( $n_e \sim 0.6 \times 10^{19} \text{ m}^{-3}$ ). The mode frequency of each burst chirps downward from  $\sim 100 \text{ kHz}$  to  $\sim 50 \text{ kHz}$  within a short time scale less than 1 ms. The value of  $\delta B_\theta$  ranges from  $6.0 \times 10^{-5} \text{ T}$  to  $8.0 \times 10^{-5} \text{ T}$  in this case. Correlated with the EPM bursts, pulsed increases are observed in NPA, SLIP and  $H\alpha$  signals. It is noted that signals of the FLIP and DLP show similar behavior to that of the SLIP. It is seen that the evolution of NPA flux is earlier than that of the SLIP. The increase of NPA flux is a result that fast

ions are transported to the peripheral domain where the neutral hydrogen is much denser than that in the core domain. The NPA flux begins to increase right after the magnetic fluctuation begins to evolve whereas the evolution of lost fast ion flux is somewhat delayed. This is because the NPA signal contains information of fast ions in the interior region of a plasma. It should be noted that the NPA oriented to the tangential direction shows that correlated with the EPMs, the fast particle flux only in the energy range close to  $E_b$  ( $\sim 40 \text{ keV}$ ) increases periodically whereas the fluxes of partially thermalized particles do not. This suggests that fast ions transported to the edge region are not well confined [17]. These experimental observations indicate that the EPMs cause significant effects on fast ion transport, leading to rapid loss of fast ions. It is also indicated that the EPMs are stabilized after an expulsion of fast ions.

It is interesting and important to study fast ion behaviors in an interior region of plasma when EPMs are excited for understanding of interplay between the mode and fast ions. Lately, we have found that the DLP can work as a fast ion probe [15]. The DLP in CHS has multi-probe tips and is designed to be tough for the heat load so as to insert into an NB-heated plasma and



provides local information of fast ion behavior inside a plasma although information of fast

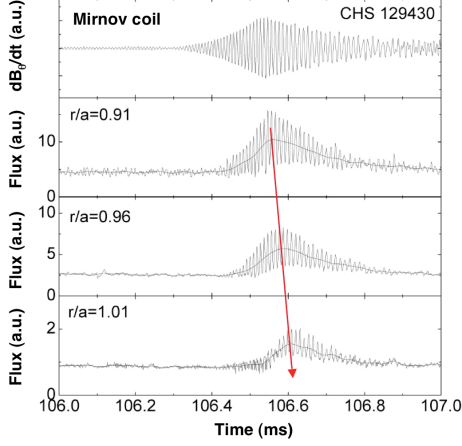


FIG. 7. Time variation of fast ion flux reaching the DLP for three different locations, i.e,  $r/a = 0.91, 0.96$  and  $1.01$  due to the EPM activities in  $B_t/R_{ax}$  of  $0.91$  T/ $0.962$  m. The red arrow line represents the trace of peak position of fast ion flux.

ions such as energy and pitch-angle is not provided. Figure 7 shows fast ion behavior at different positions in the vicinity of plasma boundary while EPMs are excited in  $B_t/R_{ax}$  of  $0.91$  T/ $0.962$  m. The interesting observation is that correlated with the magnetic fluctuations, fast ion fluxes reaching the DLP are strongly oscillated. Such a strong oscillation does not appear on signals of SLIP and FLIP placed at the outside of plasma. This is supposed to be due to results from interaction between the rotating modes and fast ions. The time-resolved fast ions transport to the peripheral region due to the EPM has been clearly seen. Velocity of radial movement of fast ions is fairly high and is

evaluated to be about  $6 \times 10^2$  m/s. The internal measurement on fast ions also suggests that fast ions transported by the EPMs escape rapidly from CHS plasmas in  $B_t$  of  $0.91$  T.

#### 4. Particle simulation with magnetic perturbation

Assuming an internal mode structure ( $m=3/n=2$ ) of EPM activities motivated by heavy ion beam probe data, we made an effort to simulate the fast particle loss by using the DELTA5D code. The result indicates that a perturbed field whose amplitude is consistent with the CHS experiment can rapidly increase the fast ion losses as compared to losses in the stationary magnetic field (Fig. 8). It was also shown that fast ion losses were strongly enhanced as the mode amplitude increases as seen in the experiments. The frequency downshift can strongly influence the fast ion confinement compared with the fixed mode frequency.

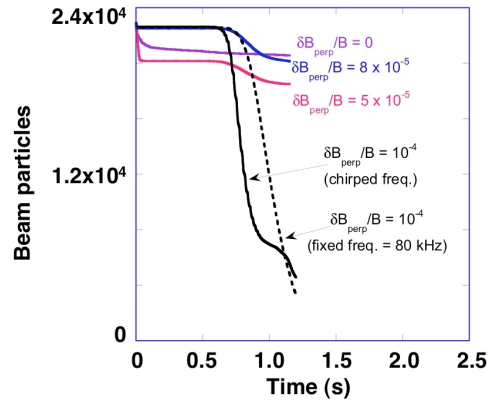


FIG. 8. Time evolution of number of confined beam ions for the different amplitude of magnetic fluctuation in the CHS configuration.

## 5. Summary

Recent results on fast-ion-driven MHD instabilities and consequent fast ion transport in a low aspect ratio helical system CHS are presented. It was shown that the  $n=1$  TAE instabilities driven by co-circulating beam ions lead to significant beam ion losses toward the outboard side of the torus. Fast ion losses are enhanced as the fluctuation amplitude of TAEs or EPMs increases. Detailed study on fast ion transport due to the EPMs ( $n/m=2/3$ ) characterized by periodic recurrence and rapid frequency downshift revealed that the effect of EPMs on fast ion confinement is significant and fast ions affected by the EPMs are rapidly lost.

## Acknowledgements

This work is supported by the CHS project budget (NIFS05ULPD609). This is also supported in part by a Grant-in-Aid for Scientific Research from JSPS No 16686051, and by a Grant-in-Aid for Scientific Research on Priority Areas from MEXT No 16082209.

## References

- [1] CHEN, L., et al., Phys. Plasmas **1** (1994) 1519-1522.
- [2] CHENG, C.Z. and CHANCE, M.S, Phys. Fluids **29** (1986) 3695-3701.
- [3] VLAD, G., et al., Nuclear Fusion **46** (2006) 1-16.
- [4] WONG, K.L., et al., Phys. Rev. Lett. **66** (1991) 1874.
- [5] HEIDBRINK, W.W., et al., Nuclear Fusion **31** (1991) 1635-1648.
- [6] SHARAPOV, S.E., et al., Nuclear Fusion **39** (1999) 373-388.
- [7] KIMURA, H., et al., Nuclear Fusion **38** (1998) 1303-1314.
- [8] ISHIKAWA, M., et al., Nuclear Fusion **46** (2006) S898-S903.
- [9] WELLER, A., et al., Phys. Rev. Lett. **72** (1994) 1220-1223.
- [10] TAKECHI, M., et al., Phys. Rev. Lett. **83** (1999) 312-315.
- [11] TOI, K., et al., Nuclear Fusion **40** (2000) 1349-1361.
- [12] YAMAMOTO, S., et al., Nuclear Fusion **45** (2005) 326-336.
- [13] ISOBE, M., et al., Rev. Sci. Instrum. **70** (1999) 827-830.
- [14] ISOBE, M., et al., Rev. Sci. Instrum. **77** (2006) 10F508-1-10F508-3.
- [15] NAGAOKA, K., et al., Plasma and Fusion Research **1** (2006) 005-1-005-2.
- [16] MATSUSHITA, H., et al., Rev. Sci. Instrum. **75** (2004) 3607-3609.
- [17] ISOBE, M., et al., Nuclear Fusion **46** (2006) S918-S925.